



**HAL**  
open science

## Influence of polar ozone loss on northern midlatitude regions estimated by a high-resolution chemistry transport model during winter 1999/2000

Marion Marchand, Sophie Godin, Alain Hauchecorne, Franck Lefèvre, Slimane Bekki, Martin Chipperfield

### ► To cite this version:

Marion Marchand, Sophie Godin, Alain Hauchecorne, Franck Lefèvre, Slimane Bekki, et al.. Influence of polar ozone loss on northern midlatitude regions estimated by a high-resolution chemistry transport model during winter 1999/2000. *Journal of Geophysical Research: Atmospheres*, 2003, 108 (D5), 10.1029/2001JD000906 . insu-03112045

**HAL Id: insu-03112045**

**<https://insu.hal.science/insu-03112045>**

Submitted on 15 Jan 2021

**HAL** is a multi-disciplinary open access archive for the deposit and dissemination of scientific research documents, whether they are published or not. The documents may come from teaching and research institutions in France or abroad, or from public or private research centers.

L'archive ouverte pluridisciplinaire **HAL**, est destinée au dépôt et à la diffusion de documents scientifiques de niveau recherche, publiés ou non, émanant des établissements d'enseignement et de recherche français ou étrangers, des laboratoires publics ou privés.

## Influence of polar ozone loss on northern midlatitude regions estimated by a high-resolution chemistry transport model during winter 1999/2000

Marion Marchand, Sophie Godin, Alain Hauchecorne, Franck Lefèvre, and Slimane Bekki

Service d'Aéronomie, Université de Pierre et Marie Curie, Paris, France

Martyn Chipperfield

School of the Environment, University of Leeds, Leeds, UK

Received 30 May 2001; revised 6 November 2001; accepted 30 November 2001; published 22 January 2003.

[1] The Modèle Isentropique de transport Mésoéchelle de l'Ozone Stratosphérique par Advection avec CHIMie (MIMOSA-CHIM) three-dimensional high-resolution chemical transport model has been developed to estimate the contribution of polar ozone destruction to the lower stratosphere ozone budget at midlatitudes. The ability of the model to reproduce the evolution of polar and midlatitude ozone during the 1999/2000 winter is first evaluated by comparisons against lidar and sonde measurements. The modeled potential vorticity (PV) fields are also compared with PV fields derived from ECMWF analyses and the chemical fields of the model are compared with the output of a large-scale chemical transport model in order to highlight the interest of a high-resolution model for resolving fine-scale structures such as polar filaments. A PV-based analysis is performed to estimate the area covered by polar air, vortex, and filaments in the 45°N–55°N latitude band at 475K and their contribution to ozone loss. The polar air contribution was found to represent usually between 20% and 40% of the total ozone loss in this latitude band but can reach 50% during large vortex intrusions. At 475K, the total chemical ozone loss in nonpolar air between 45°N and 55°N increases from 1% in mid-December to 15% at the end of March. Several chemical ozone tracers are considered to investigate the origin of the ozone loss in nonpolar air. These tracers allow us to quantify the amount of chemical ozone destruction that occurred in the vortex, in the polar filamentary structures, and in the nonpolar air. Until February, the main contributor to the nonpolar ozone loss is in situ destruction at midlatitudes, but the contribution from the ozone destruction in the polar vortex increases steadily during the winter and represents about 50% of the total midlatitude ozone loss in April, after the vortex breakup. The contribution from the ozone destruction within filamentary structures is found to be quasi-negligible as a result of the limited number of filaments. *INDEX TERMS*: 3334 Meteorology and Atmospheric Dynamics: Middle atmosphere dynamics (0341, 0342); 0341 Atmospheric Composition and Structure: Middle atmosphere—constituent transport and chemistry (3334); 0340 Atmospheric Composition and Structure: Middle atmosphere—composition and chemistry; *KEYWORDS*: polar filament, midlatitude, ozone loss, irreversible transport, chemical ozone loss

**Citation:** Marchand, M., S. Godin, A. Hauchecorne, F. Lefèvre, S. Bekki, and M. Chipperfield, Influence of polar ozone loss on northern midlatitude regions estimated by a high-resolution chemistry transport model during winter 1999/2000, *J. Geophys. Res.*, 108(D5), 8326, doi:10.1029/2001JD000906, 2003.

### 1. Introduction

[2] It is now well recognized that recent decades have seen a decline of the total ozone column in northern midlatitudes [*World Meteorological Organization (WMO)*, 1999]. Reported ozone trends are larger in the winter spring seasons (4%/decade) than in the summer autumn seasons (2%/

decade). The main contribution to the total ozone trends is located in the 12–20 km altitude range [*Harris et al.*, 1997].

[3] In contrast with polar ozone destruction which is attributed to anthropogenic emissions of chlorofluorocarbons (CFCs) [*Molina and Rowlands*, 1974], the origin of the midlatitude ozone decline still remains an open question. Several hypothesis have been proposed. They range from in situ chemistry, involving heterogeneous reactions on aerosol [*Hoffman and Solomon*, 1989], changes in the intensity of the Brewer-Dobson circulation leading to an effect on

diabatic descent [Randel and Cobb, 1994], and the transport of ozone-poor air or polar stratospheric cloud (PSC)-activated air from the polar vortices toward midlatitudes [Waugh *et al.*, 1994; Orsolini, 1995].

[4] This paper focuses on the last proposed mechanism which involves the transport of polar air toward midlatitudes. The polar vortex is relatively isolated from the midlatitude region, but air parcels can be peeled off the vortex edge and mixed with midlatitude air throughout the winter and spring seasons [Plumb *et al.*, 1994]. Waugh *et al.* [1994] estimated that, for January 1992, around 40% of the vortex was transported to midlatitudes. Small-scale vertical structures, or laminae of depleted or enriched in ozone have been observed in ozone sonde measurements for many years [Dobson, 1973; Reid and Vaughan, 1991]. Reid and Vaughan [1991] found that ozone laminae were most common in winter and spring near the polar vortex edge in the lower stratosphere, with layers typically one kilometer thick. The polar vortex edge is deformed by the meridional wind induced by planetary Rossby waves breaking [McIntyre and Palmer, 1984], leading to the formation of polar air filaments that are afterward stretched by the meridional gradient of zonal wind. Polar air is transported to midlatitudes in these filaments and ultimately mixed with the surrounding air by small-scale dynamical processes [Waugh *et al.*, 1994].

[5] Such a mechanism may have several effects. First, it leads to transport of polar air which is poorer or richer in ozone compared to the surrounding midlatitude air. Second, this polar air may also be chemically activated: the stretching of filaments from the polar night to sunlit midlatitudes leads then to in situ ozone depletion.

[6] Some of the filament processes, such as dissipation and mixing with the surrounding air, are small-scale processes which are not fully resolved in meteorological analyses and therefore require high-resolution models. Different techniques such as reverse domain-filling trajectories [Orsolini *et al.*, 1997], contour advection with surgery [Waugh *et al.*, 1994; Mariotti *et al.*, 1997] and high-resolution potential vorticity (PV) advection [Hauchecorne *et al.*, 2002] are now able to represent the observed filaments down to scales of a few tens of kilometers.

[7] The present paper focuses on the effect of transport of polar air on the lower stratospheric ozone budget at midlatitudes for the Arctic winter 1999/2000. A three-dimensional high-resolution chemical transport model has been developed in order to estimate the amount of polar ozone loss transported to midlatitudes and quantify its contribution to the midlatitude ozone decline. The high-resolution model is described in section 2. Section 3 presents an evaluation of the ability of the model to simulate ozone chemistry in polar and midlatitude regions. A case study of polar filament is discussed in section 4. The amount of polar chemical ozone loss transported toward midlatitudes is also estimated. In section 5, the model is used to quantify the contribution of polar air, with distinction between vortex and filaments, to the ozone budget at midlatitudes. Section 6 is devoted to a summary of the results and conclusions.

## 2. Description of the Chemical Transport Model

[8] The three-dimensional high-resolution chemical transport model called Modèle Isentropique de transport Mésos-

échelle de l'Ozone Stratosphérique par Advection avec CHIMie (MIMOSA-CHIM) has been developed to study the role of small-scale transport processes in determining the chemical composition of the stratosphere. The chemistry scheme originates from the Reactive Processes Ruling the Ozone Budget in the Stratosphere (REPROBUS) model [Lefèvre *et al.*, 1994]. The ability of the MIMOSA dynamical model to describe filamentary structures through the advection of potential vorticity (PV), as a quasi-passive tracer, has been already evaluated during comparisons against airborne lidar measurements within the framework of the METRO project [Hauchecorne *et al.*, 2002; Heese *et al.*, 2001], and against observations of ozone laminae on lidar profiles at the Observatoire de Haute Provence (OHP, 44N-6E) [Godin *et al.*, 2002].

[9] The model uses an isentropic vertical coordinate (surfaces of constant potential temperature) with ten levels between 350K and 950K, resulting in a vertical resolution of approximately 2 km in the lower stratosphere. The model horizontal resolution used for this study is  $1^\circ$  latitude  $\times$   $1^\circ$  longitude. The model domain is centered onto the North Pole and covers the Northern Hemisphere down to  $30^\circ$ N in the present version. The model is forced by temperature, pressure and wind fields provided by ECMWF (European Centre for Medium-Range Weather Forecasts) daily analyses. Since the lifetime of filaments are 10 days typically, the daily analyses are sufficient to resolve the temporal evolution of the filaments. The spatial resolution of the meteorological analyses is  $2.5^\circ \times 2.5^\circ$ , corresponding to the T42 truncation. In order to take into account fluxes from regions below the  $30^\circ$ N latitude, PV fields of the ECMWF analyses and REPROBUS chemical fields are used to force this boundary of the model. PV forcing occurs daily. Since the REPROBUS chemical fields are available every 10 days, they are interpolated in time for the forcing. In order to initialize the model at the beginning of the simulation, the PV fields provided by the ECMWF analyses and the REPROBUS chemical fields are interpolated linearly onto the finer MIMOSA-CHIM horizontal grid.

[10] The ECMWF daily winds are used to advect chemical species and PV, with a time step of 1 h. The advection scheme is semi-Lagrangian. The original orthogonal grid is stretched and deformed by horizontal gradients in the wind field. It is necessary to re-interpolate the advected model fields onto the original grid in order to conserve the distance between two adjacent grid points. The interpolation onto the original grid is performed every 6 h. This regridding process induces a numerical diffusion which is minimized by an interpolation scheme based on the preservation of the second order moments of the PV and chemical species distributions [Hauchecorne *et al.*, 2002].

[11] It is necessary to take into account the diabatic vertical transport across isentropic surfaces for simulations larger than a few days. The radiation scheme used to calculate the heating rates is taken from the SLIMCAT model [Chipperfield, 1999] and was initially developed by Shine [1987] and Shine and Rickaby [1989]. Ozone and water vapor fields used in the radiative calculations are climatologies. It must be pointed out that the heating rates calculated by the radiative scheme are not adjusted to ensure global mass balance (i.e., globally integrated vertical mass fluxes on isentropic surfaces is not null). This correction

could not be included because the meteorological analyses were only available to us over the Northern Hemisphere. The radiation scheme uses dummy levels between the MIMOSA-CHIM isentropic levels and the heating rates are calculated every day. The vertical scheme is based on the mass fluxes estimation on these dummy levels to calculate cross isentropic the diabatic transport. The diabatic evolution of PV is taken into account by relaxing the model PV toward the PV calculated from the ECMWF fields with a relaxation time of 10 days. It is assumed that, at least for the larger scales, diabatic changes of PV are accounted for in the evolution of the ECMWF PV fields.

[12] The chemical scheme is taken from the REPROBUS CTM [Lefèvre *et al.*, 1994]. The stratospheric chemistry is comprehensive and the scheme contains an heterogeneous chemistry module which takes into account liquid super-cooled aerosols, as well as NAT and ice particles. In order to determine the cumulative ozone loss during the integration, a ozone passive tracer was also implemented in the model. This tracer is initialized in the same way as ozone at the beginning of the winter and is then advected passively without any production and loss term. The time step for integrating the chemistry is 15 min.

[13] The model chemistry was initialized on 13 December 1999 from a REPROBUS chemical simulation. The simulations ran continuously until 30 April 2000. high-resolution PV and chemical fields were stored at 0000 and 1200 UT every day.

### 3. Model Validation

[14] The first objective of developing the high-resolution model is to quantify the effect of transport of polar air on lower stratospheric ozone at midlatitudes. With this aim in mind, the description of polar and midlatitude ozone by the model needs to be validated. Such a validation was performed for the Arctic region. Figure 1 presents a comparison between the ozone sonde measurements at Ny-Ålesund (79°N, 12°E) and the model values from December 1999 to late March 2000 at 435K and 475K. The movement of the polar vortex with respect to the station is determined by comparing the potential vorticity at the station with the potential vorticity at the outer edge of the vortex. This movement can be divided in two periods. From December 1999 to 16 March 2000 (day 76), the measurements are mostly taken inside the vortex core with some short periods when the edge of the vortex is scanned. In the second part of the winter, from 16 March to the end of March, the station is alternately at the edge, outside the vortex and sometimes within filamentary structures. This is well reflected in the time series of the ozone mixing ratio showing large variations during that period. This offers us the opportunity to describe the evolution of ozone within the polar vortex during the activation period and to contrast it with the evolution of ozone at midlatitudes.

[15] From December 1999 to mid-January, the evolution of polar ozone at 435K and 475K should be largely controlled by the diabatic descent of ozone from above. During this period, our model MIMOSA-CHIM tends to calculate ozone values below the measurements and the REPROBUS values until the end of January, especially at

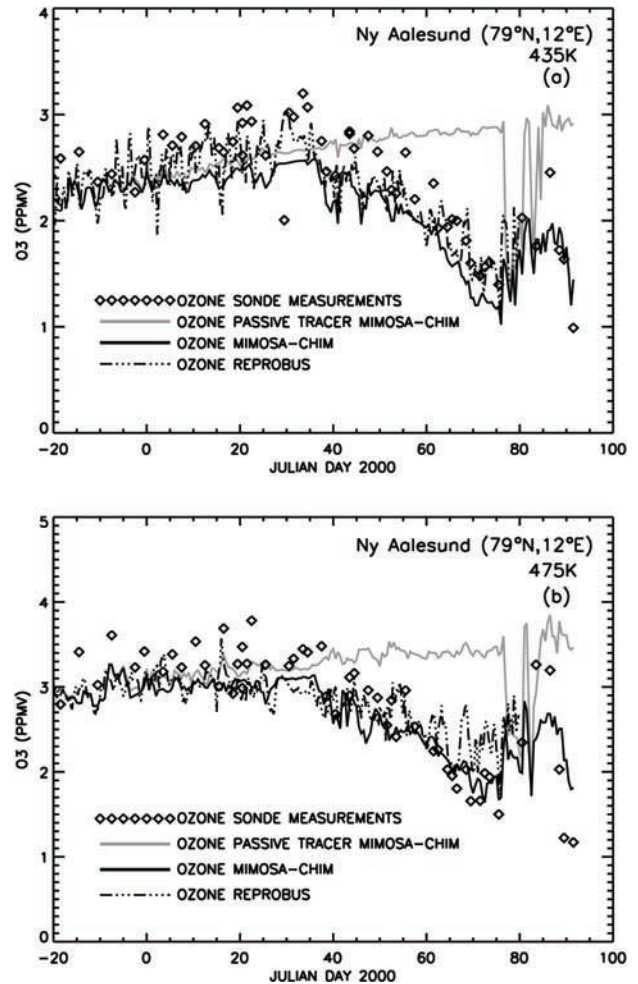


**Figure 1.** Temporal evolution of ozone mixing ratio at Ny-Ålesund (79°N, 12°E) during winter 2000. Comparison between the ozone sondes measurement and the ozone calculated by the MIMOSA-CHIM model ( $1^\circ \times 1^\circ$ ) and the REPROBUS CTM ( $2^\circ \times 2^\circ$ ) at (a) 435K and at (b) 475K.

435K. At this level the diabatic descent rate in REPROBUS was found to be accurate when compared to the SAGE III—Ozone Loss and Validation Experiment and Third European Stratospheric Experiment on Ozone 2000 (SOLVE/THE-SEO) measurements [Greenblatt *et al.*, 2002]. Therefore the difference between both models suggests that MIMOSA-CHIM somewhat underestimates the diabatic subsidence at the beginning of the winter, when it is strongest at 435K. This bias is being investigated and may be related to the relatively low vertical resolution of MIMOSA-CHIM, the low-order vertical advection scheme, or improper global mass balance in the model.

[16] The chlorine activation (not shown) starts in the model around day 40 with ClO mixing ratio rapidly reaching values of 1.2 ppbv at 435K and 1.5 ppbv at 475K. The model reproduces reasonably well the slope of the ozone decline observed over Ny-Ålesund from day 40 until day 75 (mid-March) at 435K and 475K. At 435K, however, the insufficient diabatic descent at the beginning of the winter leads to ozone values that are systematically lower than the measurements by about 0.4–0.5 ppmv. By comparing the

ozone passive tracer and the model ozone, the chemical ozone loss, which should strictly be called net chemical ozone change, is estimated to reach about 1.7 ppmv at 435K and 1.8 ppmv (about 50% loss) at 475K by 12 March 2000. This range is in good agreement with other estimates obtained using different methods [Rex *et al.*, 2000; Sinnhuber *et al.*, 2000; Braathen *et al.*, 2000; Deniel *et al.*, 2000].

[17] The REPROBUS model tends to underestimate the ozone loss in late February/early March especially at 475K in the vortex. The contrast between polar and midlatitude air is also not large enough between day 80 and day 90. The differences between the ozone simulations of the MIMOSA-CHIM and REPROBUS models are likely to be due to the differences in resolution. The high resolution, with the reduced diffusion, used in MIMOSA-CHIM reduces the horizontal mixing through the vortex edge. As a result, the strong ozone gradients occurring at the vortex edge toward the end of the winter are better preserved in the MIMOSA-CHIM simulations than in the REPROBUS simulations. The larger diffusion in the REPROBUS model leads to non-activated midlatitude air getting into the vortex. This mixing inhibits the destruction of polar ozone and flattens the contrast between polar and midlatitude ozone.

[18] In order to validate the model ozone behavior at midlatitudes, Figure 2 compares lidar ozone measurements at the Observatoire de Haute Provence (OHP, 44°N, 6°E) and the MIMOSA-CHIM and REPROBUS models at 435K and 475K. REPROBUS results are only shown at the dates of the lidar measurements, whereas the temporal resolution of MIMOSA-CHIM is two values per day. The ozone lidar measurements are performed using the DIAL method [Godin *et al.*, 1989], and provide a relatively large sampling of the ozone field with around 15 measurements per month. Overall, the temporal evolutions of ozone simulated by both models compares well with the measurements. At 435K, the differences in ozone between the REPROBUS and MIMOSA-CHIM simulations range, on average, 15% and 7%, respectively. At 475K, these differences are about 6% and 4%, respectively, between REPROBUS and MIMOSA-CHIM. Because of the stability of the vortex in winter 2000, the passage of polar filaments, or of the polar vortex itself, was relatively rare above the OHP station. One filament and a vortex intrusion occurred in early and mid-March as revealed by sharp increases in PV values over the OHP station at 475K. The vortex had started to break up during that period. The MIMOSA-CHIM simulations indicate a chemical ozone loss over the OHP station varying from 1% to 12% at 435K and 1% to 15% at 475K during the winter. A peak ozone loss of about 30% is predicted on 3 March 2000 at 475K, corresponding to the vortex intrusion over the station.

#### 4. Resolving Small-Scale Features With High-Resolution Modeling

[19] Small-scale structures like filaments are often not fully resolved in large-scale models. This could represent a potentially significant source of error in establishing the ozone budget, especially at midlatitudes. High-resolution advection models are more able to resolve the very fine structures present in PV and chemical fields. In principle, they should reduce spurious mixing and better preserve the

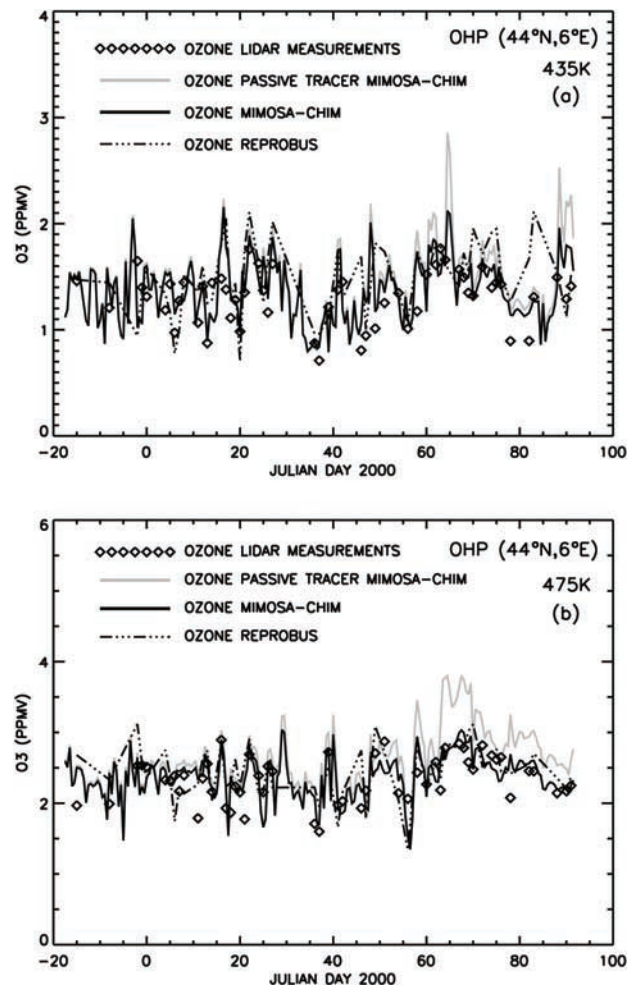


**Figure 2.** Temporal evolution of ozone mixing ratio at OHP (44°N, 6°E) during winter 2000. Comparison between the ozone lidar measurement and the ozone calculated by the MIMOSA-CHIM model ( $1^\circ \times 1^\circ$ ) and the REPROBUS CTM ( $2^\circ \times 2^\circ$ ) at (a) 435K and at (b) 475K.

gradients in the fields. In addition, averaging and mixing can affect calculated chemical rates. Edouard *et al.* [1996] found a very strong dependency of the calculated polar ozone loss on the model resolution by comparing simulations of a single layer model run at varying resolutions. They attributed this high sensitivity to the averaging of small-scale variability in ozone-destroying ClO. However, results from other studies suggested that their results were model-dependent. Tan *et al.* [1998] also showed that predicted ozone loss rates are sensitive to model resolution in the regime relevant to current large-scale models (i.e., 100 km or more), but that sensitivity decreases considerably once the resolution is less than 100 km. Sparling *et al.* [1998] analyzed high-resolution aircraft ClO data over scales ranging from 50 to 800 km. They found that calculated ozone loss rate due to the ClO dimer cycle can be in error by as much as about 40% at the vortex edge when averaging the data over 800 km. Small errors (less than 10%) were found inside the vortex. Searle *et al.* [1998a, 1998b] found little sensitivity of the calculated polar ozone loss on the model resolution in chemical transport model simulations integrated at resolutions ranging

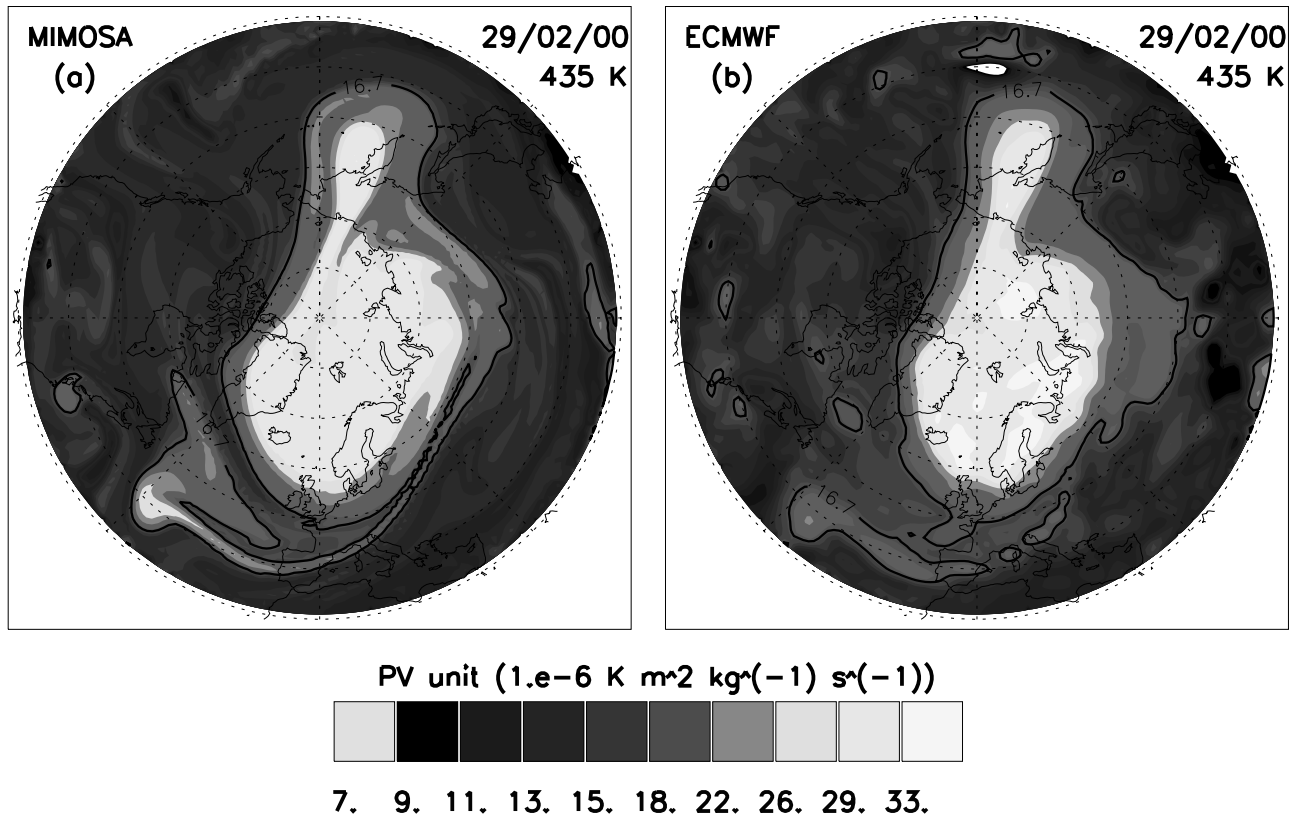


**Figure 3.** Potential vorticity on 2 February 2000 at 435K. Comparison between (a) the PV field advected by MIMOSA ( $1^\circ \times 1^\circ$ ) and (b) the ECMWF analyses ( $2.5^\circ \times 2.5^\circ$ ). (PV expressed in pv unit.)

from 80 to 300 km. Their results demonstrated that, under conditions of moderate to large chlorine activation within the vortex, the effects of averaging on calculated polar ozone loss are necessarily small. The issue of model resolution becomes more important for a weakly activated vortex. These results suggest that the spatial averaging of small-scale features plays a minor role in the strong sensitivity of calculated polar ozone loss to model resolution found by *Edouard et al.* [1996]. It seems likely that the main cause lies within resolution-dependent transport or mixing across the vortex edge accompanied by chlorine deactivation. All the studies mentioned above focus on the effects of model resolution on polar ozone loss. The effect of model resolution and, in particular, resolving polar filaments, on calculated midlatitude ozone loss is still an unresolved issue. In order to illustrate the interest of the MIMOSA-CHIM model for the study of polar structures and their chemical effects, a case study of polar filament on 29 February 2000 at 435K is presented here.

[20] Figure 3 shows a comparison between PV fields calculated from the ECMWF analyses at  $2.5^\circ$  horizontal resolution and by the MIMOSA-CHIM model at  $1^\circ$  resolution. The “advected” PV field reproduced by a transport model represents better the filament structure of polar air than the “dynamical” PV field computed directly using meteorological variables. MIMOSA-CHIM shows the development of a filamentary structure on that day, with a large tongue of polar air extends from the edge of the vortex over Siberia to the northern Atlantic at about  $40N$  latitude. High-PV blobs are only visible along the filament in the

large-scale ECMWF analyses. These features do not appear to be connected to the core of the vortex. The resolution does not allow us to follow accurately the thin filament stretching toward midlatitudes.

[21] Figure 4 shows, for the same day and the same isentropic level as Figure 3, the comparison between chemical ozone loss fields provided by the MIMOSA-CHIM model and by the REPROBUS models. The MIMOSA-CHIM resolution is again twice as high as the REPROBUS resolution. The filament is characterized by chemical ozone loss values which are characteristic of the inside or the edge of the vortex. Only the end of the filament is clearly visible in the REPROBUS ozone loss field. The MIMOSA-CHIM numerical diffusion is likely to be stronger than the true stratospheric diffusivity. However, it remains smaller than in CTMs like REPROBUS. The high resolution allows us to track better the ozone loss within the nearly full extent of the filament. MIMOSA-CHIM predicts on that day ozone losses between 15% and 30% inside the filament whereas they range between 10% and 20% in REPROBUS. These differences can be explained, on one hand, by different losses within the vortex, and, on the other hand, by a better representation of the small-scale filamentation processes at the vortex edge in MIMOSA-CHIM. In addition, the better preservation of the gradients at the edge of the filamentary structure in MIMOSA-CHIM reduces the effect of mixing on the chemical composition of the filament during its transport toward midlatitudes.

[22] The filament of 29 February 2000 originated at the edge of the vortex in mid-February. At that time, the vortex

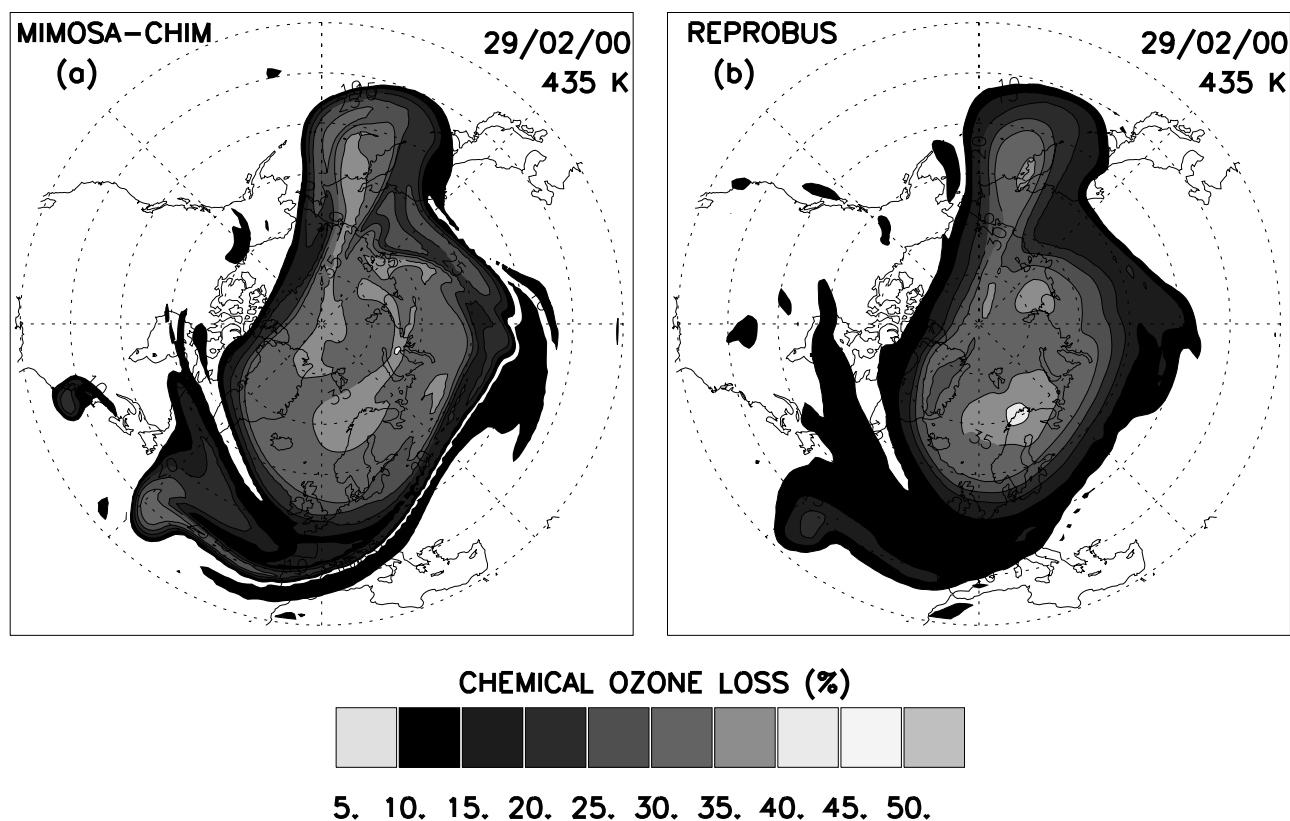


**Figure 4.** Accumulated chemical ozone loss (percent relative to the passive ozone tracer) on 2 February 2000 at 435K. Comparison between (a) MIMOSA-CHIM ( $1^\circ \times 1^\circ$ ) and (b) REPROBUS ( $2^\circ \times 2^\circ$ ).

elongated toward lower latitudes over Eastern Siberia, with accumulated ozone loss up to 25% (relative to the ozone passive tracer) at 435K and by a maximum in ClO of about 0.7 ppbv. A few days later, this elongation of the vortex formed a tongue of polar air characterized by ozone loss up to 35% and ClO mixing ratios of around 0.8 ppbv. The ClO amounts decreased during the stretching and thinning of the tongue, eventually reaching values of around 0.1 ppbv.

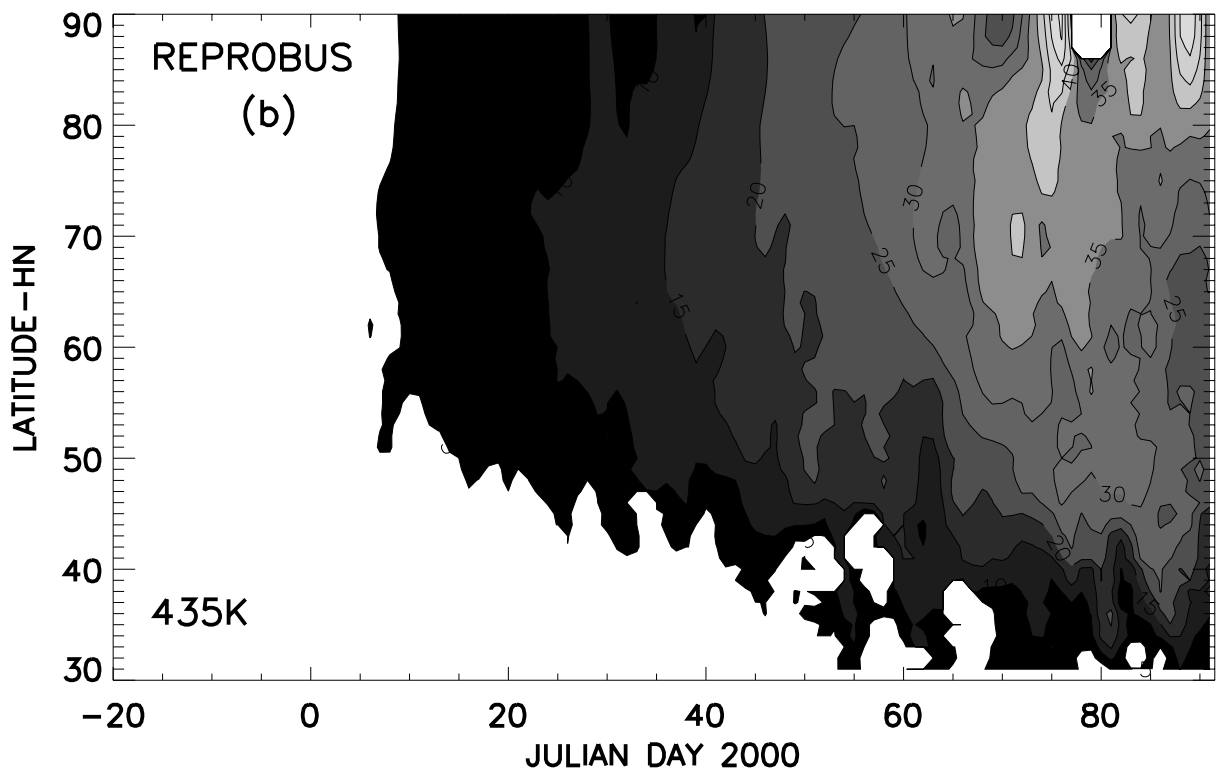
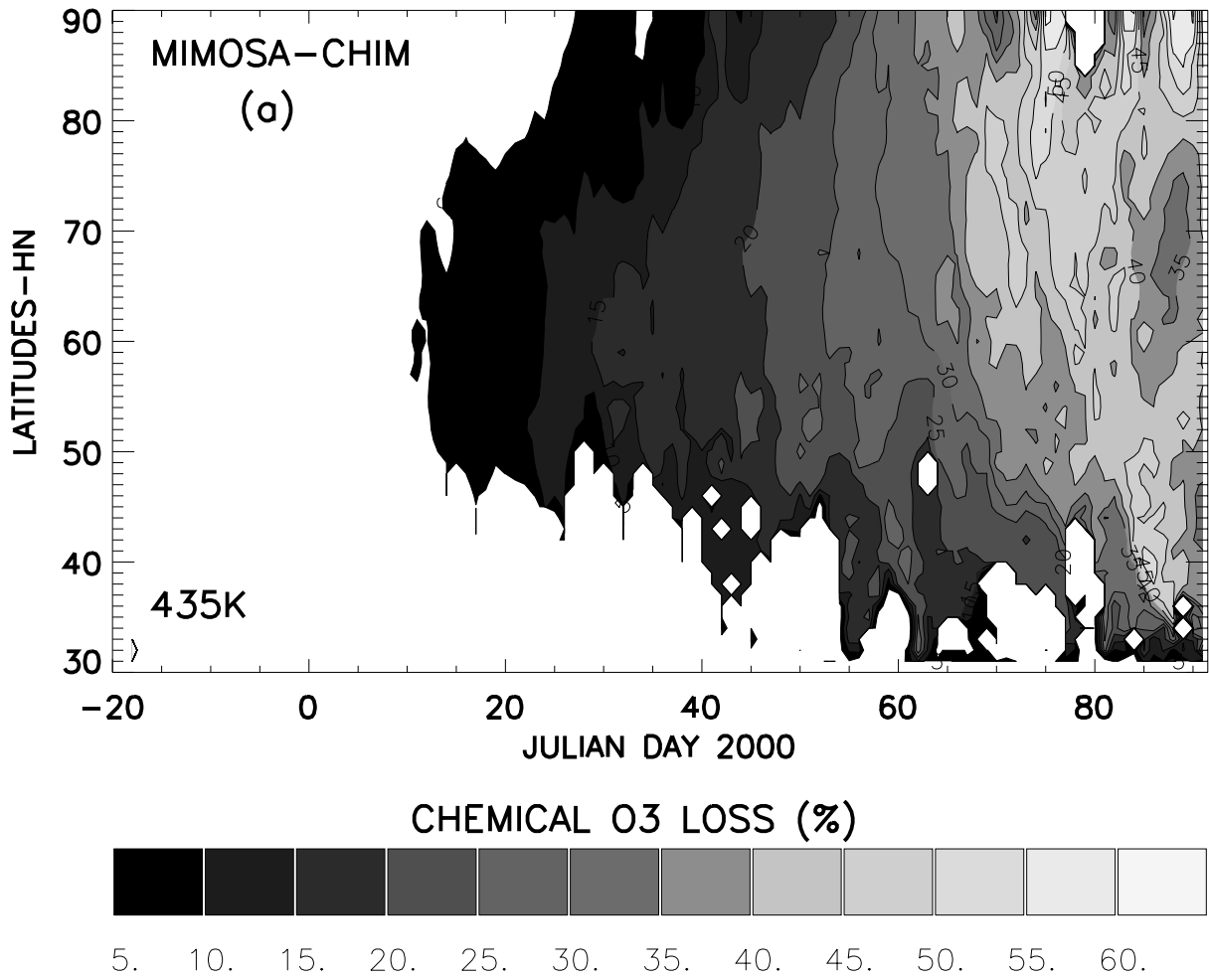
[23] The MIMOSA-CHIM simulation is now compared to the REPROBUS simulation on an hemispheric scale to estimate the amount of polar ozone loss reaching the mid-latitudes during the 2000 Arctic winter. The temporal evolution of polar ozone at 435K along geographical latitudes is shown for both models in Figure 5. Polar ozone is defined following the PV criterion of *Nash et al.* [1996], based on the second derivative of the PV expressed as a function of equivalent latitude [*McIntyre and Palmer, 1984; Butchart and Remsberg, 1986*]. We define as polar air the parcels included in the inner vortex and at the vortex edge. This method has already been used with success in the classification of ground-based ozone measurements obtained inside, outside and at the edge of the Antarctic polar vortex [*Godin et al., 2001*] and for the detection of vortex intrusions and filament passages over the OHP station [*Godin et al., 2002*]. The polar ozone loss value defined as the difference

between the passive ozone tracer and the chemical ozone, and is averaged along geographical latitude bands of  $1^\circ$ . Since the vortex was stable in 2000 with a low number of filaments, the percentage of polar air at midlatitudes is similar in the high-resolution MIMOSA-CHIM simulation and in the ECMWF analysis. Little polar air is found at 435K at midlatitudes from mid-December to mid-January. The evolution of polar ozone loss at midlatitudes is relatively similar in both models with values reaching 25% at the beginning of March. From mid-March, differences between the models are more pronounced, and polar ozone is then destroyed at a faster rate in MIMOSA-CHIM. The chemical ozone loss reaches 50% in MIMOSA-CHIM whereas it only peaks at 35% in REPROBUS. The polar ozone loss also appears to spread to lower latitudes in the high-resolution MIMOSA-CHIM simulation. These differences suggest that, once the vortex starts breaking up, mixing between polar and midlatitudes air is faster in REPROBUS, leading to a more rapid chlorine deactivation and lower polar ozone losses.

## 5. Influence of Polar Air on Ozone at Midlatitudes

[24] The transport of polar air toward midlatitudes occurs through the extension of filament toward lower latitudes and

**Figure 5.** (opposite) Temporal evolution of the chemical ozone loss in polar air (percent related to the passive ozone tracer) during winter 2000 at 435K as a function of latitude. Comparison between (a) MIMOSA-CHIM ( $1^\circ \times 1^\circ$ ) and (b) REPROBUS ( $2^\circ \times 2^\circ$ ).



through vortex intrusions. This transport can have two effects whether it is reversible or irreversible. If reversible, the effect is to perturb the ozone content at midlatitudes during a limited period of time. If irreversible, polar air is mixed with the surrounding air, leading to permanent ozone changes in midlatitude air. This aspect of the transport has already been considered by *Knudsen and Grooß* [2000], who estimated a vortex dilution of 2.6% of the 1979 ozone column in May 1997. In the first part of this section, the role of transport of polar air toward midlatitude is evaluated considering both the reversible and irreversible aspects. In the second part, only the irreversible aspect of this transport is considered.

### 5.1. Effect of Transport of Polar Air Toward Midlatitudes

[25] A method is developed to distinguish three types of air: Air inside the vortex, air within filaments, or nonpolar air located outside the vortex, using the same PV threshold as in section 4.

[26] In the case of polar air, vortex air and filaments are distinguished according to the PV variation between the considered polar air parcel and the center of the vortex. Essentially, we look for the vortex outer edge (defined by the PV threshold) along the line connecting the considered parcel to the center of the vortex (defined by the maximum PV). If the vortex outer edge is found along this line, the air parcel is considered to be within a filament. Tongues and parts of a very distorted vortex are identified as filaments. Therefore the method gives an upper limit for the amount of air within filaments.

[27] From mid-December to the end of March 2000, the proportion of nonpolar air at 475K for latitudes greater than 35°N varies between 65% and 78%; the proportion of polar air varies between 22% and 34%. The surface occupied by filaments is found to be negligible until mid-February (smaller than 2%). Then, it increases to 5% from mid-February to mid-March and finally represents 15% at the end of March when the vortex starts breaking up (no figure shown). These low values of filament air reflects the stability of the vortex during the 1999/2000 winter with a relatively small number of filaments. Compared to the four last winter (from 1996 to 2000), the winter 1999/2000 was characterized by the smaller number of polar detection above the OHP station [*Godin et al.*, 2002]. Using the method described above, the polar and nonpolar fractions of the 45°N–55°N latitude band is plotted as a function of time in Figure 6a. Figure 6a shows that this geographical latitude band at 475K is mainly representative of nonpolar air with values ranging from 70% to 97% of the total surface area. However, the polar air fraction increases during the winter and peaks at 32% on 7 March. The polar contribution within this latitude band is decomposed into vortex and filament air in Figure 6b. This figure reveals that polar air mostly corresponds to vortex intrusions until mid-February. Then the proportion of filament air becomes very significant and, as expected, largely dominates after the vortex breaks up at the end of the winter. On average, during the winter, air in filaments and inside the vortex represents 5% and 10% of the 45°N–55°N air, respectively.

[28] Each intrusion of polar air into midlatitudes leads to a transport of chemical ozone loss characteristic of vortex

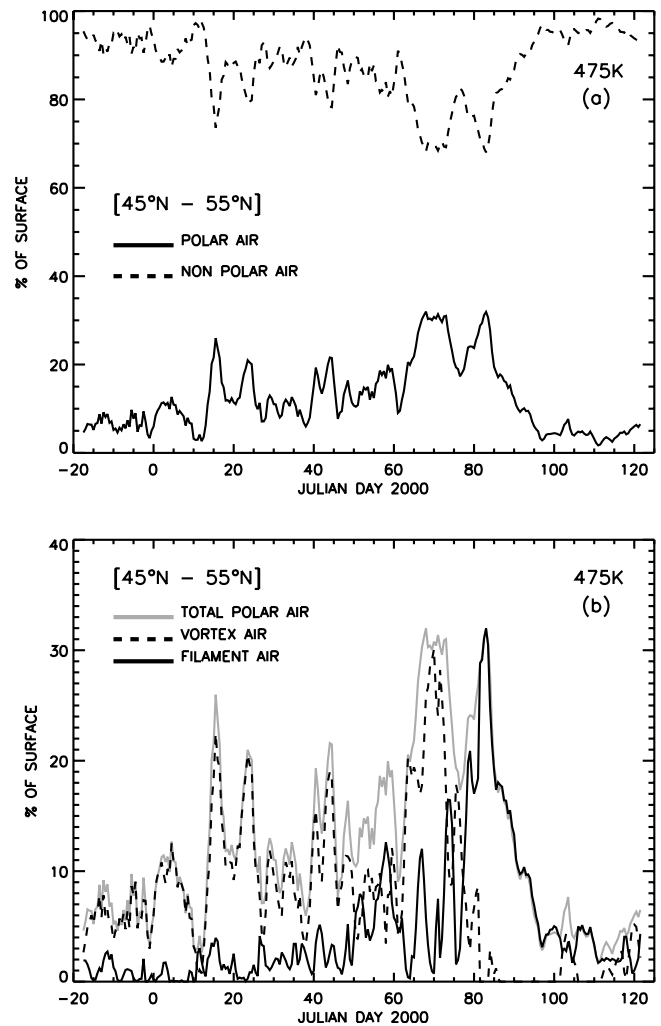


**Figure 6.** Fractional surface of nonpolar (dashed line) at 475K and polar (solid line) air in the 45°N–55°N latitude band from 13 December 1999 to 30 April 2000. (b) Fractional surface of total polar air (solid grey) at 475K, vortex (dashed black) and filament (solid black) air in the 45°N–55°N latitude band from 13 December 1999 to 30 April 2000.

air. In order to quantify the effect of this transport, the total cumulative chemical ozone loss within this midlatitude band ( $O3L_{total}$ ) is estimated from

$$O3L_{total} = \frac{\sum_{i,j} O3L_{i,j} * SURF_{i,j}}{\sum_{i,j} SURF_{i,j}} \quad (1)$$

where ( $SURF_{i,j}$ ) is the surface area of the grid box, indexes  $i$  and  $j$  refer to latitude and longitude respectively, and  $O3L_{i,j}$  is defined as

$$O3L_{i,j} = \frac{O3tracer_{i,j} - O3_{i,j}}{O3tracer_{i,j}} \quad (2)$$

where ( $O3tracer_{i,j}$ ) and ( $O3_{i,j}$ ) are the mixing ratios of the passive ozone tracer and the chemically active ozone, respectively.

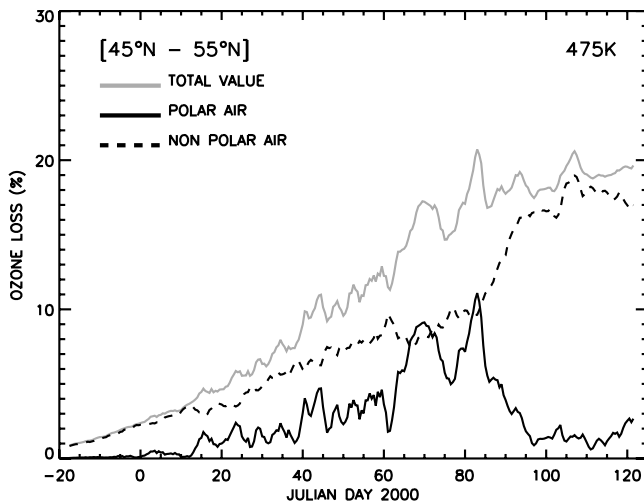


**Figure 7.** Accumulated ozone loss at 475K averaged in the 45°N–55°N latitude band from 13 December 1999 to 30 April 2000. Solid grey: total loss. Dashed black: contribution of nonpolar air. Solid black: contribution of polar air.

[29] The respective contributions of nonpolar and polar air to the total ozone loss can easily be estimated from

$$O3L_{total} = \frac{\sum_{i,j(polar)} O3L_{i,j} * SURF_{i,j}}{\sum_{i,j} SURF_{i,j}} + \frac{\sum_{i,j(nonpolar)} O3L_{i,j} * SURF_{i,j}}{\sum_{i,j} SURF_{i,j}} \quad (3)$$

[30] The temporal evolution of the chemical ozone loss between 45°N and 55°N is represented in Figure 7. The loss increases until the end of March from 1% to 18%, with an average rate of 0.2%/day. The ozone loss evolution is also subject to fluctuations linked to polar intrusions with larger ozone loss values. Indeed, typical polar ozone loss values within this latitude band can reach 20% to 30% from February to the end of March. Even if the transport of polar air in this region is associated with high values of ozone loss, its contribution to the total ozone loss is relatively limited due to the low frequency and small surface area of such intrusions. Overall, the contribution of polar air represents 20% to 40% of the total loss from mid-January to the end of February. During the large vortex intrusions of March, up to 50% of the ozone loss is attributed to polar air. The ozone loss within nonpolar air between 45°N and 55°N also tends to increase until the end of March from 1% to 15%. Several hypotheses can be put forward to explain this evolution of the nonpolar ozone loss. Among them lies in situ midlatitude chemical loss [Cahill *et al.*, 2000], and the irreversible transport by filaments and vortex intrusions, which is quantified in the following section.

## 5.2. Effect of Irreversible Transport of Polar Air

[31] The analysis in the previous section does not distinguish between the effects of reversible and irreversible transport of polar air toward midlatitudes. For instance, polar intrusions affect only temporarily the ozone content at midlatitudes. In order to understand the origin of ozone loss in nonpolar air, it is necessary to track the chemical

ozone losses within the three types of air/domains defined in our study: nonpolar, filaments, and vortex. For this purpose, several chemical ozone tracers were included in the model. They are advected in the same way as the other chemical species and are modified by chemistry only within the specific domains they represent. In practice, the chemical ozone change of a given air parcel (grid point) over a 12 h interval is added to the chemical ozone tracer corresponding to the air/domain of this air parcel. Since three regions are considered, there are nine potential types of dynamical evolution. There are three cases corresponding to the evolution within the three regions without transitions and six cases corresponding to the transitions

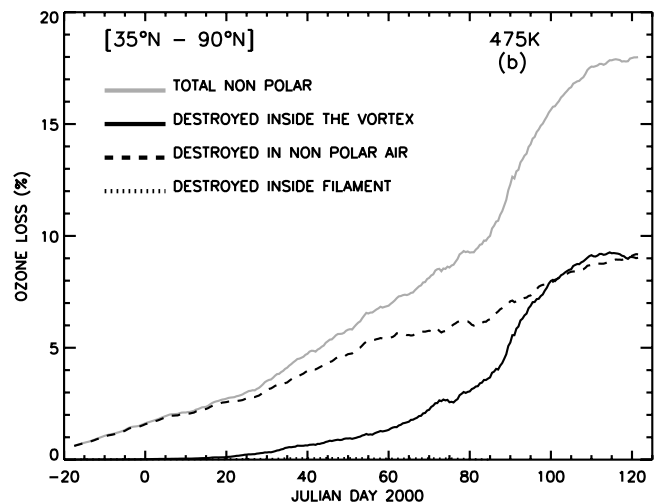
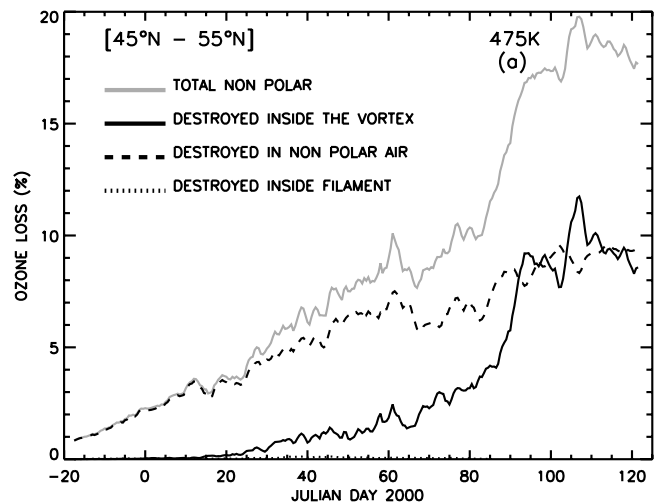


**Figure 8.** (a) Accumulated ozone loss at 475K in nonpolar air, averaged in the 45°N–55°N latitude band from 13 December 1999 to 30 April 2000. Solid grey: total nonpolar ozone loss. Dashed black: part destroyed in nonpolar air. Solid black: part destroyed inside the vortex. Dotted black: part destroyed inside filament. (b) Accumulated ozone loss at 475K in nonpolar air, averaged in the 35°N–90°N latitude band from 13 December 1999 to 30 April 2000. Dashed black: part destroyed in nonpolar air. Solid black: part destroyed inside the vortex. Dotted black: part destroyed inside filament.

between the three regions (total number of combinations). Since it is possible for an air parcel to move from one of the three domains to another over a 12 h interval, nine chemical ozone tracers are included in the model instead of 3; the additional six ozone tracers correspond to the possible transitions from one domain to another. As expected, throughout the winter integration, the sum of the chemical ozone tracers changes is equal to the total chemical ozone change at every grid point of the model, even if the contribution of the six ozone tracers corresponding to the transitions represents a negligible part of the overall destruction. This method allows us to determine where chemical ozone losses in nonpolar air originate from. For example, it is possible to quantify the amount of ozone destroyed in filament or vortex air which is subsequently transported to the nonpolar domain.

[32] The contribution of the three domains (where the ozone has been destroyed) to the ozone loss in nonpolar air between  $45^{\circ}\text{N}$  and  $55^{\circ}\text{N}$  (already plotted in Figure 7) is plotted on Figure 8a. Indeed, only nonpolar air must be considered here to quantify the contribution of the irreversible transport of polar air to ozone loss at midlatitudes. As mentioned in section 5.1, the ozone loss in nonpolar air between  $45^{\circ}\text{N}$  and  $55^{\circ}\text{N}$  increases from 1% to 15% until the end of March (see Figure 8a). Until February, the main cause for ozone loss in nonpolar air is nonpolar (in situ) chemical processes. Then, the contribution of ozone destruction occurring inside the vortex starts to increase sharply. This behaviour is associated with the stability of the vortex and with the state of the ozone destruction inside the vortex. By the end of March, this contribution becomes almost comparable to the nonpolar destruction. The contribution of ozone destruction in filaments is very small. It is important to stress again that filaments were relatively rare in 2000 because of the relatively strong stability of the polar vortex. However, this does not rule out the potentially important role of filaments in the irreversible transport of polar air into midlatitudes. Indeed, this irreversible transport of vortex parcel can be associated both to the direct transfer from the vortex to nonpolar air and can also arise through filaments. The latter transfer explains 50% of this irreversible transport until mid-March and more than 80% at the end of April. In April, the vortex falls to pieces and its surface area decreases very rapidly. The fraction of polar air within the midlatitude band becomes negligible (see Figure 6a) and its contribution to ozone loss follows the same pattern (see Figure 7). However, due to the large dilution of the vortex, the contribution of ozone destruction inside the vortex to the total ozone loss at midlatitudes is comparable in April to the in situ (nonpolar) destruction, as shown in Figure 8a. In order to understand the increase of the contribution of destruction occurring into nonpolar air, a preliminary study of the ozone-destroying cycles has been made. The  $\text{HO}_x$  cycle are the most important in nonpolar air. The second most important cycles are the halogen and  $\text{NO}_x$  cycles which operate most effectively at the beginning and at the end of the winter respectively.

[33] For a more global view of the midlatitudes, the total ozone loss in nonpolar air is now integrated over latitudes greater than  $30^{\circ}\text{N}$ . The temporal evolution of the ozone loss and of its three components are shown in Figure 8b. The curves are smoother than in Figure 8a as polar intrusions

and filaments do not move out of the considered domain. However, the overall picture does not change substantially compared to the results obtained for the limited latitude band of  $45^{\circ}\text{N}$ – $55^{\circ}\text{N}$ : Our study shows that, at the end of the winter 1999/2000, irreversible transport from the vortex contributed as much as in situ chemical loss to the ozone destruction in midlatitudes.

## 6. Summary

[34] A three-dimensional high-resolution chemical transport model MIMOSA-CHIM has been developed to estimate the contribution of the transport of polar air to the ozone loss at midlatitudes. The model couples the high-resolution advection model MIMOSA with a radiation scheme and with a full chemistry package. MIMOSA-CHIM was integrated to study the dynamical and chemical evolution of polar filaments during the 1999/2000 winter. The model simulations have been validated against ozone sonde and lidar measurements at high and midlatitudes. The comparisons show a reasonably good agreement, although the diabatic descent in the polar region is found to be slightly underestimated at the beginning of the winter, especially at 435K. The high-resolution simulations ( $1^{\circ} \times 1^{\circ}$ ) were then compared to the PV fields derived from ECMWF analysis ( $2.5^{\circ} \times 2.5^{\circ}$ ) and with a large-scale simulation of the REPROBUS CTM ( $2^{\circ} \times 2^{\circ}$ ). The MIMOSA-CHIM model preserves better the gradients in the chemical and PV fields at the edge of the polar structures, the filaments and the polar vortex. It also preserves better the integrity of the chemical composition within the filaments, particularly during stretching toward midlatitudes. Chemical ozone loss inside polar air advected toward midlatitudes, is higher in the MIMOSA-CHIM simulation than in the large-scale REPROBUS simulation during the 1999/2000 winter at 435K. A PV-based analysis is used to estimate the area covered by polar air, vortex, and filaments in the  $45^{\circ}\text{N}$ – $55^{\circ}\text{N}$  latitude band, and their contribution to ozone loss. The polar air contribution was found to represent usually 20% and 40% of the total ozone loss in this latitude band, but can reach 50% during large vortex intrusions.

[35] In order to understand the origin of the ozone loss in nonpolar air, several chemical ozone tracers were included in the model. These tracers monitor the amount of chemical ozone destruction in the vortex, in polar filamentary structures and in nonpolar air. At 475K, the total chemical ozone loss in nonpolar air between  $45^{\circ}\text{N}$  and  $55^{\circ}\text{N}$  increases from 1% in mid-December to 15% at the end of March. Until February, the main contributor to the ozone loss is in situ destruction in nonpolar air. However, the contribution from the ozone destruction in the vortex increases steadily during the winter, and exceeds 40% of the total loss by the end of March. In April, the total chemical ozone loss stabilizes at 18%–20% within the  $45^{\circ}\text{N}$ – $55^{\circ}\text{N}$  latitude band. Although polar air is rare during this period, the contribution from the ozone destruction that took place in the polar vortex is comparable to the nonpolar destruction. The overall picture does not change much when the results are integrated on the larger  $35^{\circ}\text{N}$ – $90^{\circ}\text{N}$ : By the end of the winter, the ozone destruction that occurred in the vortex, followed by irreversible transport and mixing, contributed to as much as 50% of the ozone reduction in midlatitudes.

[36] The contribution from the ozone destruction within filamentary structures is found to be quasi negligible, as a result of the limited number of filaments and the high stability of the 1999/2000 Arctic winter. However, the results highlighted in this paper suggest, as a perspective, the study of a more disturbed winter which was characterized by a larger number of filaments, as observed in 1997–1998 and a detailed estimation of catalytic cycles contributions to chemical ozone loss observed in midlatitudes.

[37] **Acknowledgments.** The authors wish to thank the whole lidar team at the Observatoire de Haute-Provence for the ozonolidar measurements and at the Ny-Ålesund for the ozone sondes measurements. We thank ECMWF and NILU for providing meteorological data. This work was supported by EC contract METRO ENV4-CT97-0520.

## References

- Braathen, G., et al., Temporal evolution of ozone in the Arctic vortex during winters from 1988–89, *Proc. 5th Eur. Symp. on Polar Ozone Air Pollut. Res. Rep. 73*, edited by N. R. P. Harris, M. Guirlet, and G. T. Amanatidis, pp. 411–416, Eur. Comm., 2000.
- Butchart, N., and E. Remsburg, The area of the stratospheric polar vortex as a diagnostic for tracer transport on an isentropic surface, *J. Atmos. Sci.*, **43**, 1319–1339, 1986.
- Cahill, G. A., A. M. Lee, and J. A. Pyle, Quantification of the polar contribution to mid-latitude ozone loss, in *Proceedings of the Quadrennial Ozone Symposium*, pp. 205–206, Int. Ozone Comm., Int. Assoc. for Meteorol. and Atmos. Sci., Sapporo, Japan, 3–8 July 2000.
- Chipperfield, M. P., Multiannual simulation with a three-dimensional chemical transport model, *J. Geophys. Res.*, **104**, 1781–1806, 1999.
- Deniel, C., et al., Arctic ozone loss deduced by POAM, *Proc. 5th Eur. Symp. on Polar Ozone Air Pollut. Res. Rep. 73*, edited by N. R. P. Harris, M. Guirlet, and G. T. Amanatidis, pp. 421–424, Eur. Comm., 2000.
- Dobson, G. M. B., The laminated structure of ozone in the atmosphere, *Q. J. R. Meteorol. Soc.*, **99**, 599–607, 1973.
- Edouard, S., B. Legras, F. Lefèvre, and R. Eymard, The effect of small-scale in homogeneities on ozone depletion in the Arctic, *Nature*, **384**, 444–447, 1996.
- Godin, S., G. Mégie, and J. Pelon, Systematic measurements of the stratospheric ozone vertical distribution, *Geophys. Res. Lett.*, **16**, 547–550, 1989.
- Godin, S., V. Bergeret, S. Bekki, C. David, and G. Mégie, study of the interannual ozone loss and the permeability of the Antarctica polar vortex from long-term aerosol and ozone lidar measurements in Dumont d'Urville (66.4°S, 140°E), *J. Geophys. Res.*, **106**, 1311–1330, 2001.
- Godin, S., M. Marchand, A. Hauchecorne, and F. Lefèvre, Influence of Arctic polar ozone depletion on lower stratospheric ozone amounts at Haute-Provence Observatory (43.92°N, 5.71°E), *J. Geophys. Res.*, **107**(20), 8272, doi:10.1029/2001JD000516, 2002.
- Greenblatt, J. B., et al., Tracer-based determination of vortex descent in the 1999/2000 Arctic winter, *J. Geophys. Res.*, **107**(20), 8279, doi:10.1029/2001JD000937, 2002.
- Harris, N. R. P., et al., Trends in stratospheric and free tropospheric ozone, *J. Geophys. Res.*, **102**, 1571–1590, 1997.
- Hauchecorne, A., S. Godin, M. Marchand, B. Heese, and C. Souprayen, Quantification of the transport of chemical constituents from the polar vortex to middle latitudes in the lower stratosphere using the high-resolution advection model MIMOSA and effective diffusivity, *J. Geophys. Res.*, **107**, doi:10.1029/2001JD000491, in press, 2002.
- Heese, B., S. Godin, and A. Hauchecorne, Forecast and simulation of stratospheric ozone filaments: A validation of a high-resolution potential vorticity advection model by airborne ozone lidar measurements in winter 1998/1999, *J. Geophys. Res.*, **106**, 20,011–20,024, 2001.
- Hoffman, D. J., and S. Solomon, Ozone destruction through heterogeneous chemistry following the eruption of El Chichon, *J. Geophys. Res.*, **94**, 5029–5041, 1989.
- Knudsen, B. M., and J.-U. Grooß, Northern midlatitude stratospheric ozone dilution in spring modeled with simulated mixing, *J. Geophys. Res.*, **105**, 6885–6890, 2000.
- Lefèvre, F., G. P. Brasseur, I. Folkins, A. K. Smith, and P. Simon, Chemistry of the 1991/1992 stratospheric winter: Three-dimensional model simulations, *J. Geophys. Res.*, **99**, 8183–8195, 1994.
- Mariotti, A., M. Moustouai, B. Legras, and H. Teitelbaum, Comparison between vertical ozone, sounding and reconstructed potential vorticity maps by contour advection with surgery, *J. Geophys. Res.*, **102**, 6131–6142, 1997.
- McIntyre, M. E., and T. N. Palmer, The “surf zone” in the stratosphere, *J. Atmos. Terr. Phys.*, **9**, 825–849, 1984.
- Molina, M. J., and F. S. Rowlands, Stratospheric sink for chlorofluoromethanes: Chlorine atom-catalysed destruction of ozone, *Nature*, **249**, 810–812, 1974.
- Nash, E. R., P. A. Newman, J. E. Rosenfield, and M. E. Schoeberl, An objective determination of the polar vortex using Ertel's potential vorticity, *J. Geophys. Res.*, **101**, 9471–9478, 1996.
- Orsolini, Y. J., On the formation ozone laminae at the edge of the Arctic polar vortex, *Q. J. R. Meteorol. Soc.*, **121**, 1923–1941, 1995.
- Orsolini, Y. J., G. Hansen, U.-P. Hoppe, G. L. Manney, and K. H. Fricke, Dynamical modeling of wintertime lidar observations in the Arctic: Ozone laminae and ozone depletion, *Q. J. R. Meteorol. Soc.*, **123**, 785–800, 1997.
- Plumb, R. A., D. W. Waugh, R. J. Atkinson, P. A. Newman, L. R. Lait, M. R. Schoeberl, E. V. Browell, A. J. Simmons, and M. Loewenstein, Intrusion into the lower stratospheric Arctic vortex during the winter of 1991/1992, *J. Geophys. Res.*, **99**, 1089–1105, 1994.
- Randel, W. J., and J. B. Cobb, Coherent variations of monthly mean total ozone and lower stratospheric temperature, *J. Geophys. Res.*, **99**, 5433–5447, 1994.
- Reid, S. J., and G. Vaughan, Lamination in ozone profiles in the lower stratosphere, *Q. J. R. Meteorol. Soc.*, **117**, 825–844, 1991.
- Rex, M., R. Lehmann, R. J. Salawitch, M. L. Santee, and J. W. Waters, Theory and observations of Arctic ozone loss rates, in *Proceedings of the Quadrennial Ozone Symposium*, pp. 250–251, Int. Ozone Comm., Int. Assoc. for Meteorol. and Atmos. Sci., Sapporo, Japan, 3–8 July 2000.
- Searle, K. R., M. P. Chipperfield, S. Bekki, and J. A. Pyle, The impact of spatial averaging on calculated polar ozone loss, 1, Model experiments, *J. Geophys. Res.*, **103**, 25,397–25,408, 1998a.
- Searle, K. R., M. P. Chipperfield, S. Bekki, and J. A. Pyle, The impact of spatial averaging on calculated polar ozone loss, 2, Theoretical analysis, *J. Geophys. Res.*, **103**, 25,409–25,416, 1998b.
- Shine, K. P., The middle atmosphere in the absence of dynamical heat fluxes, *Q. J. R. Meteorol. Soc.*, **113**, 603–633, 1987.
- Shine, K. P., and J. A. Rickaby, Solar radiative heating due to absorption by ozone, in *Proceedings of Quadrennial Ozone Symposium*, pp. 597–600, A. Deepack, Hampton, Va., 1989.
- Sinnhuber, B. M., et al., Large loss of total ozone during the Arctic winter of 1999/2000, *Geophys. Res. Lett.*, **27**, 3473–3476, 2000.
- Sparling, L. C., A. R. Douglas, and M. R. Schoeberl, An estimate of the effect of unresolved structure on modeled ozone loss from aircraft observations of CLO, *Geophys. Res. Lett.*, **25**, 305–308, 1998.
- Tan, D. G. H., P. H. Haynes, A. R. MacKenzie, and J. A. Pyle, The effect of fluid-dynamical stirring and mixing on the deactivation of stratospheric chlorine, *J. Geophys. Res.*, **103**, 1585–1605, 1998.
- Waugh, D. W., et al., Transport out of the lower stratosphere Arctic vortex by Ross by wave breaking, *J. Geophys. Res.*, **99**, 1071–1088, 1994.
- World Meteorological Organization, *Scientific Assessment of Ozone Depletion, 1998*, Global Ozone Res. and Monit. Proj., Genève, 1999.
- S. Bekki, S. Godin, A. Hauchecorne, F. Lefèvre, and M. Marchand, Service d'Aéronomie, Université P.M. Curie, B. 102, 4 Place Jussieu, F-75230, Paris, Cedex, France. (slimane.bekki@aero.jussieu.fr; sophie.godin@aero.jussieu.fr; alain.hauchecorne@aero.jussieu.fr; franck.lefevre@aero.jussieu.fr; marion.marchand@aero.jussieu.fr)
- M. P. Chipperfield, School of the Environment, University of Leeds, Leeds, LS2 9JT, UK. (martyn@env.leeds.ac.uk)